GAZİOSMANPAŞA BİLİMSEL ARAŞTIRMA DERGİSİ (GBAD)
Gaziosmanpasa Journal of Scientific Research
ISSN: 2146-8168
http://dergipark.gov.tr/gbad
Araştırma Makalesi (Research Article)

Cilt/Volume : 12
Sayı/Number: 2
Yıl/Year: 2023
Sayfa/Pages: 105-114

***Alınış tarihi (Received)*:** 05.09.2023
***Kabul tarihi (Accepted)*:** 14.09.2023

Evaluating Shear Contribution of FRP To Masonry Walls

Zeynep ÜNSAL ASLAN[1,*], **Metin KARSLIOĞLU**[2]

[1] *Civil Engineering Department, Faculty of Engineering and Architecture, Tokat Gaziosmanpasa University, Tokat, TÜRKİYE,*
[2] *Civil Engineering Department, Faculty of Civil Engineering, Yıldız Technical University, İstanbul, TÜRKİYE,*
**Corresponding author: zeynepunsalaslan@gmail.com*

ABSTRACT: In earthquake-prone regions, there has been a notable focus on employing modern and efficient strengthening techniques to enhance the durability of unreinforced masonry walls (URM) in recent years. Among these approaches, the utilization of Fiber Reinforced Polymer (FRP) for strengthening has particularly gained recognition. In this paper, a novel empirical model is presented, employing nonlinear regression analysis, to forecast the shear contribution of FRP strips. URM walls with three configurations of the FRP strips have been considered: one is horizontal FRP strips, the second is vertical FRP strips, and the other is FRP grid strips. The proposed model is developed by using the input parameters determined by considering fourteen different experimental specimens available in the literature, and also considers the influence of reinforcement ratio (ρ_0), which was not taken into account in previously suggested models. The shear contribution of FRP strips was compared with the ACI 440.7R-10 model and experimental results. The essential step in any analytical model is evaluating the developed model's accuracy by comparing it with the experimental data and model. This evaluation was performed using the coefficient of determination R^2. The results indicated that the suggested model accurately forecasts the shear contribution of FRP strips and is better aligned with experimental results compared to the ACI 440.7R-10 model.

Keywords – *Unreinforced masonry wall, FRP strips, reinforcement ratio, empirical model, horizontal and vertical*

Yığma Duvarlarda FRP Kesme Dayanımı Katkısının Değerlendirilmesi

ÖZET: Deprem bölgelerinde, donatısız yığma duvarların (URM) dayanıklılığını artırmak için modern ve etkili güçlendirme tekniklerin kullanılmasına yönelik son yıllarda dikkate değer bir ilgi oluşmuştur. Bu yaklaşımlar arasında Fiber Takviyeli Polimerin (FRP) güçlendirme amacıyla kullanılması oldukça kabul görmektedir. Bu yayında, doğrusal olmayan regresyon analizi kullanılarak, FRP şeritlerinin kesme dayanımı katkısını tahmin eden yeni bir ampirik bağıntı sunulmuştur. FRP şeritler ile güçlendirmede üç farklı konfigürasyon dikkate alınmıştır. Bu konfigürasyonlardan biri yatay FRP şeritlerinin, ikincisi dikey FRP şeritlerinin ve diğeri hem yatay hem dikey FRP şeritlerin birlikte kullanıldığı konfigürasyondur. Önerilen model, literatürde yer alan on dört farklı deney numunesi dikkate alınarak belirlenen girdi parametreleri kullanılarak geliştirilmiştir. Ayrıca, önerilen modelde literatürde mevcut modellerde dikkate alınmayan güçlendirme oranının (ρ_0) etkisi de dikkate alınmıştır. FRP şeritlerin kesme dayanımı katkısı ACI 440.7R-10 modeli ve deneysel sonuçlarla karşılaştırılmıştır. Herhangi bir analitik modelin değerlendirilmesindeki temel adım, geliştirilen modelin doğruluğunu deneysel veriler ve modelle karşılaştırarak değerlendirmektir. Bu değerlendirme belirleme katsayısı (R^2) kullanılarak yapılmıştır. Sonuçlar, önerilen modelin FRP şeritlerin kesme dayanımı katkısını doğru bir şekilde tahmin ettiğini ve ACI 440.7R-10 modeline kıyasla deneysel sonuçlarla daha iyi uyumlu olduğunu göstermiştir.

Anahtar Kelimeler – *Donatısız yığma duvar, FRP şeritleri, güçlendirme oranı, ampirik model, yatay ve dikey*

1. Introduction

The recent earthquakes have demonstrated once again the poor seismic vulnerability of unreinforced masonry (URM) walls. It also showed the necessity of strengthening these walls in order to prevent the damage caused by this weakness. There are various traditional methods, such as shotcrete, grout injection, and external reinforcement, as well as modern techniques like Fiber Reinforced Polymer that are currently employed to strengthen URM walls (Doran et al., 2022). Strengthening with FRP is preferred more than conventional techniques due to its benefits such as lower weight than other structural system, low cost construction, rapid application, prevention from corrosion and no loss of valuable space (Marshall et al., 2000; ElGawady et al., 2004a; Elgawady et al., 2004b; Moon et al., 2007; Marcari et al., 2011; Vega and Torres, 2018; Cheng et al., 2020; Emami et al., 2020; Doran et al., 2022;). Over the years, extensive research campaigns have been conducted to examine the role of FRP in enhancing the shear strength of URM walls. However, compared to experimental and numerical research, little information exists in the literature for analytical research. The assumption is made that the total shear strength (V_n) of masonry walls strengthened with FRP consists of the combined shear strength of the URM wall (V_m) and the additional shear contribution provided by the FRP (V_f). Over the last twenty years, several analytical models have been developed to determine the amount of shear contribution of FRP. Triantafillou (1998) suggested a model specifically designed for situations where FRP strips are in the shape of narrow straps, in order to estimate the impact of FRP. Triantafillou and Antonopoulos (1999) developed a model that takes into account various failure modes of FRP (such as debonding or rupture) and different types of FRP materials (such as CFRP or AFRP). Garbin et al. (2007) presented an analytical model that can be used for the application of FRP in both vertical and horizontal orientations. The CNR-DT 200 (CNR-DT 200,2004) code , provides a model that allows for calculating the shear contribution of FRP strips when the FRP reinforcement is positioned parallel to the mortar joints. Furthermore, the ACI 440.7R-10 code (ACI 440.7R-10,2010), offers a model that suggests a way to estimate the shear contribution provided by FRP strips when they are applied in a parallel and vertical manner to the mortar joints. Among these models for estimating shear contribution of FRP strip considering the reinforcement ratio (ρ_0), have not yet been investigated. In the scope of this study, a novel analytical model, considering the reinforcement ratio (ρ_0), has been put forth for the purpose of estimating the shear contribution of horizontal, vertical and grid FRP strips. Nonlinear regression analysis was performed using SPSS (Statistical Package for Social Science). Moreover, an extensive statistical assessment was performed to evaluate the accuracy and efficiency of the suggested model. The experimental results were more in line with the proposed model than with ACI 440.7R-10 code.

2. Material and Methods

The nominal shear strength (V_n) of a masonry wall strengthened with FRP composites can be written as:

$$V_n = V_m + V_f \quad (1)$$

where V_m stands for the nominal shear strength of URM wall and V_f stands for the FRP contribution to the nominal shear strength for FRP-strengthened masonry walls. In this study, a new analytical model has been introduced to estimate the shear contribution of FRP (V_f)

taking into account the reinforcement ratio (ρ_0). The reinforcement ratio, ρ_0, is computed as follows:

$$\rho_0 = \frac{n\, t_f w_f}{H_w t_w}\, x100 \tag{2}$$

where the number of FRP layers is referred as n; FRP thickness is defined as t_f; w_f is the total length of FRP; the height of the wall and the thickness of the wall is referred as H_w and t_w, respectively.

The input parameters used in the development of the proposed analytical equation/model were derived from an assessment of fourteen distinct experimental specimens available in the literature. In the selection of the experimental data set used in the study, attention was paid to the application of FRP strip configurations as horizontal, vertical and grid. The experimental studies conducted on masonry walls strengthened with FRP, which were considered in this study to propose analytical model, can be summarized briefly as follows. Valluzzi et al. (2002) tested solid clay brick masonry walls under in plane shear loading. CFRP, GFRP, and polyvinyl alcohol (PVAFRP) composites were used to strength masonry walls. The study explored the efficiency of FRP in various configurations, specifically focusing on its grid pattern. Additionally, the study examined how the capacity of strengthened masonry walls is affected using single-side and double-side strengthening configurations. The results indicated that using double-side configurations resulted in a more ductile failure and significantly boosted the overall capacity. Maria et al. (2006) conducted a study to assess the shear strength of URM walls made of hollow clay bricks. This was accomplished by applying external horizontal Carbon Fiber Reinforced Polymer (CFRP) strips to the walls and subjecting them to in-plane shear load. The inclusion of CFRP reinforcement had a notable impact on increasing the shear strength of the URM walls. Wang et al. (2006) conducted an experimental study on brick masonry wall strengthened by horizontal Glass Fiber Reinforced Polymer (GFRP) strips. According to results, the use of GFRP on retrofitted masonry walls enhanced the load-bearing capacity of the walls when exposed to shear loading in the plane. Marcari et al. (2007) conducted experimental study to investigate in-plane shear performance of tuff masonry walls. The panels were strengthened with GFRP and CFRP. Essentially, two distinct arrangements of FRP reinforcement were employed, including diagonal and grid layouts. The scholars determined that incorporating high-density FRP alters the failure mode from axial-rigidity failure to modes involving shear or shear-flexure. The specimens did not experience an enhancement in their elastic stiffness as a result of applying FRP. The increase in strength was accomplished without an increase in the capacity to withstand inelastic deformation. In most cases, it was observed that GFRP was better suited for with masonry walls. Martinelli et al. (2016) investigated the impact of various configurations of externally applied CFRP strips on clay brick masonry walls. These configurations are vertical, horizontal, grid, and diagonal CFRP strips. The experimental study revealed that the diagonal arrangement of these strips was the most successful in enhancing both force and displacement capabilities. Rahman and Ueda (2016) investigated the performance of clay brick masonry walls strengthened with horizontal, vertical, diagonal, and grid CFRP and polyethylene terephthalate-FRP (PET-FRP) strips. The results showed a significant rise in the in-plane shear capacity of masonry walls by using both types of FRPs. The properties of experimental specimens are given in Table 1.

Table 1. Properties of experimental specimens

Reference	Specimen	Configuration	Type
Maria et al. (2006)	CA-FH-02	Horizontal	CFRP
	CA-FH-04	Horizontal	CFRP
Wang et al. (2006)	GW2	Horizontal	GFRP
Valluzzi et al. (2002)	PR-Carb-D	Grid	CFRP
	PR-Glass-D	Grid	GFRP
	PR-PV-D	Grid	PVAFRP
Marcari et al. (2007)	C3	Grid	CFRP
	C4	Grid	CFRP
	G3	Grid	GFRP
	G4	Grid	GFRP
Martinelli et al. (2016)	H-SMW	Horizontal	CFRP
	V-SMW	Vertical	CFRP
	G-SMW	Horizontal	CFRP
Rahman and Ueda (2016)	CSG	Grid	CFRP

The specifications and attributes of these specimens are detailed in Table 2. Drawing from the experimental outcomes reported in the available literature, it is obviously seen that the estimation of the shear contribution of the FRP is primarily influenced by key parameters that were used to develop the analytical model.

Table 2. The specifications and attributes of experimental specimens

Specimens	Tensile Strength (f_f) (Mpa)	Elastic modulus (E_f) (Mpa)	Thickness of FRP (t_f) (mm)	Width (w_f) (mm)	Total number of strip (n_f)	Reinforcement ratio (ρ_0) (%)	Height (H_w) (mm)	Length (L_w) (mm)	Thickness (t_w) (mm)	Contribution of FRP (V_f^{exp}) (N)
CA-FH-02	3500	230000	0.13	150	6	0.042	2000	1975	140	86100
CA-FH-04	3500	230000	0.13	100	6	0.028	2000	1975	140	79600
GW2	1507	93750	0.169	100	6	0.056	750	1500	240	36200
PR-Carb-D	3430	230000	0.165	12	6	0.019	510	510	120	3400
PR-Glass-D	1700	65000	0.115	30	12	0.068	510	510	120	14300
PR-PV-D	1400	29000	0.07	55	24	0.151	510	510	120	47600
C3	3450	230000	0.167	200	6	0.024	1570	1480	530	66200
C4	3450	230000	0.167	200	12	0.048	1570	1480	530	88400
G3	1320	66000	0.11	200	6	0.016	1570	1480	530	64200
G4	1320	66000	0.11	200	12	0.032	1570	1480	530	83000
H-SMW	4830	230000	0.166	200	6	0.069	1160	1160	250	196300
V-SMW	4830	230000	0.166	200	6	0.069	1160	1160	250	157800
G-SMW	4830	230000	0.166	100	12	0.069	1160	1160	250	109500
CSG	3400	245000	0.111	250	14	0.371	872	1270	120	77500

Table 3 provides explanations of the statistical criteria corresponding to each input and output parameter. Table 4 presents the correlation matrix of the required parameters.

Table 3. Statistical criteria of input/output parameters

	Minimum	Maximum	Mean	Standard deviation	Skewness	Kurtosis
V_f^{exp} (N)	3400	196300	79292.86	51258.99	0.856	1.155
f_f (MPa)	1320	4830	3033.36	1341.78	-0.092	-1.41
E_f (MPa)	29000	245000	171767.86	84459.05	-0.744	-1.548
t_f (mm)	0.07	0.169	0.14	0.03	-0.701	-0.467
w_f (mm)	12	250	142.64	75.56	-0.457	-1.141
n_f	6	24	9.57	5.21	1.762	3.637
ρ_0	0.016	0.371	0.08	0.09	2.961	9.497
H_w (mm)	510	2000	1208.00	524.03	0.018	-1.205
L_w (mm)	510	1975	1260.71	479.68	-0.396	-0.405
t_w (mm)	120	530	276.43	174.47	0.756	-1.249

Table 4. Correlation matrix of input/output parameters

	V_f^{exp} (N)	f_f (MPa)	E_f (MPa)	t_f (mm)	w_f (mm)	n_f	ρ_0	H_w (mm)	L_w (mm)	t_w (mm)
V_f^{exp} (N)	1	0.671	0.441	0.318	0.611	-0.206	0.035	0.372	0.307	0.155
f_f (MPa)	0.671	1	0.899	0.643	0.235	-0.346	0.046	0.209	0.134	-0.173
E_f (MPa)	0.441	0.899	1	0.644	0.299	-0.447	0.103	0.337	0.323	-0.122
t_f (mm)	0.318	0.643	0.644	1	0.102	-0.664	-0.378	0.108	0.179	0.187
w_f (mm)	0.611	0.235	0.299	0.102	1	-0.188	0.278	0.517	0.546	0.57
n_f	-0.206	-0.346	-0.447	-0.664	-0.188	1	0.515	-0.433	-0.489	-0.179
ρ_0	0.035	0.046	0.103	-0.378	0.278	0.515	1	-0.365	-0.186	-0.394
H_w (mm)	0.372	0.209	0.337	0.108	0.517	-0.433	-0.365	1	0.894	0.464
L_w (mm)	0.307	0.134	0.323	0.179	0.546	-0.489	-0.186	0.894	1	0.347
t_w (mm)	0.155	-0.173	-0.122	0.187	0.57	-0.179	-0.394	0.464	0.347	1

Equation (3) defines the proposed model designated as V_f^{anl} to calculate the shear contribution of FRP.

$$V_f^{anl} = 102.35(1-\rho_0)^{1.223} \times \left(f_f \times t_f \times n \times w_f\right)^{0.524} - 3.13 \times 10^{-6}\left(E_f \times t_w \times L_w\right) + 1.21 \times 10^{-6}\left(E_f \times t_w \times H_w\right) - 7.9 \times 10^{-5}\left(E_f \times \varepsilon_f \times t_w \times H_w\right) + 1.87 \times 10^{-4}\left(E_f \times \varepsilon_f \times t_w \times L_w\right) \quad (3)$$

3. Results and Discussion

The performance of the suggested model can be evaluated by utilizing and the coefficient of determination (R^2). The definition of each criterion is provided by Equation (4).

$$R^2 = \frac{\left[\sum_{i=1}^{n}(exp - \overline{exp})(model - \overline{model})\right]^2}{\sum_{i=1}^{n}(exp - \overline{exp})^2 \sum_{i=1}^{n}(model - \overline{model})^2} \quad (4)$$

where, ' n ' indicates the total number of specimens, '*exp*' and '$\overline{exp}$ ' represent the actual output and the average of the actual output values, respectively. Both the *model* and the $\overline{model}$ also designate the expected output and the average of the expected outputs, correspondingly.

Figure 1 showcases a comparison of the outcomes achieved from both the experimental and proposed models.

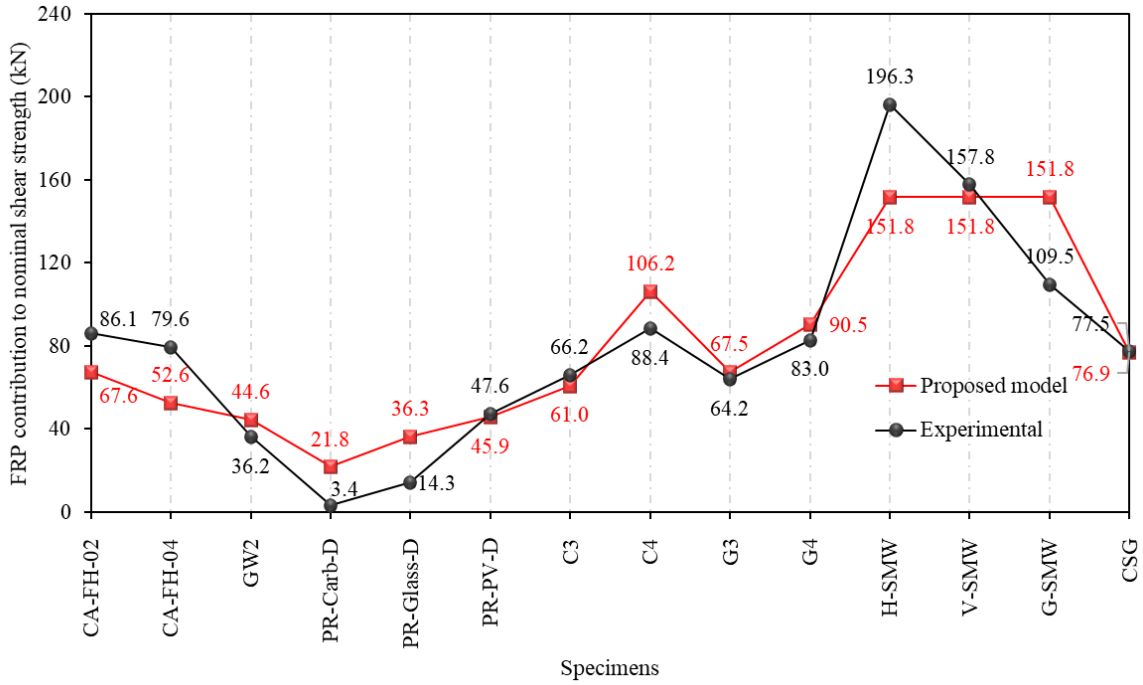

Figure 1. Comparison of proposed model and experimental results

Significantly, there is a slight difference between the results of the experiments and the results obtained from the proposed model, which is supported by an R^2 value of 0.82. It can be seen that the results of the proposed model are in good accuracy with the experimental outcomes.

In this study, the shear contribution of FRP is evaluated by comparing it with the results obtained from the ACI 440.7R-10 model, which is a code-based model. In ACI 440.7R-10 FRP shear contribution is given by Equation 5.

$$V_f = p_{fv} w_f \frac{d_v}{s_f};\ p_{fv} = n t_f f_{fe} \tag{5}$$

where, w_f represents the width of the FRP strips, d_v represents the actual depth of the masonry in the direction of shear force, s_f indicates the spacing between each strip, n refers to the number of layers of FRP strips, and f_{fe} denotes the effective stress. One way to represent the effective stress f_{fe} is by expressing it as (ACI 440.7R-10,2010):

$$f_{fe} = E\varepsilon_{fe} = E_f \kappa_v \varepsilon_{fu} = E\kappa_v C_E \varepsilon_{fu}^* \tag{6}$$

where, E_f represents the elastic modulus of FRP strips, ε_{fu}^* symbolizes the ultimate rupture strain of the FRP, and C_E is the environmental reduction factor considered to be equal to 1 for conducting the comparison with experimental outcomes. The provided value for the coefficient related to shear-controlled failure modes, κ_v, is expressed as (ACI 440.7R-10,2010):

$$\kappa_v = \begin{cases} 0.40 & for\ \omega_f \leq 0.20 \\ 0.64 - 1.2\omega_f & for\ 0.20 < \omega_f \leq 0.45 \\ 0.10 & for\ \omega_f > 0.45 \end{cases} \quad (7)$$

with ω_f in SI units equal to:

$$\omega_f = \frac{1}{85}\frac{A_f E_f}{A_n\sqrt{f'_m}} \quad (8)$$

where A_f represents the area of the external reinforcement made of FRP, A_n denotes the area of the masonry wall, and f_m' indicates the specified strength of the masonry in compression (ACI 440.7R-10,2010).

The R^2 values of the proposed model were compared with ACI 440.7R-10 model in Figure 2. It is noticed that the proposed model acquires the slightly high precision compared with the ACI 440.7R-10 model.

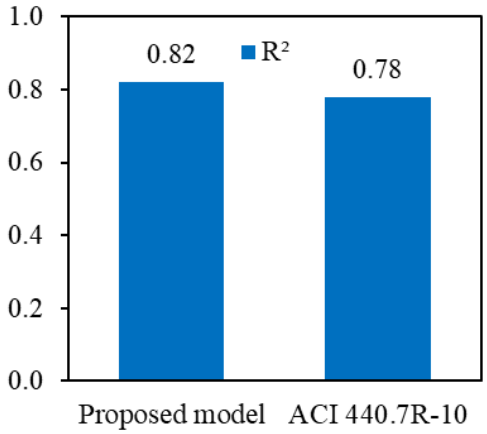

Figure 2. Evaluating the suggested and current analytical models

Figure 3 illustrates the graphical representation of the comparison between the influence of FRP on nominal shear strength, as estimated using the proposed model and the established code-based model, for each individual test specimen. The evidence clearly shows that the outcomes of the suggested model closely match the experimental findings in comparison to the ACI 440.7R-10 model.

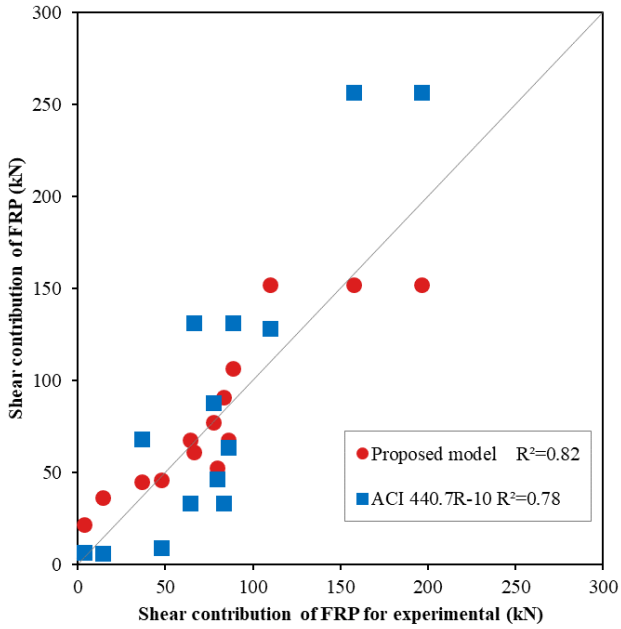

Figure 3. Comparison of the R^2 values of the proposed and existing models for each experimental specimen

The shear contribution of FRP (V_f) values of proposed model were compared with those of experimental results and ACI 440.7R-10 results (Table 5).

Table 5. Comparison of results obtained from equations and experiments

Specimens	V_f^{exp} (kN)	V_f^{ACI} (kN)	V_f^{anl} (kN)
CA-FH-02	86.1	63.4	67.6
CA-FH-04	79.6	46.4	52.6
GW2	36.2	67.9	44.6
PR-Carb-D	3.4	6.3	21.8
PR-Glass-D	14.3	5.7	36.3
PR-PVA-D	47.6	9.2	45.9
C3	66.2	131.2	61.0
C4	88.4	131.2	106.2
G3	64.2	33.1	67.5
G4	83	33.1	90.5
H-SMW	196.3	256.6	151.8
V-SMW	157.8	256.6	151.8
G-SMW	109.5	128.3	151.8
CSG	77.5	87.7	76.9

The shear contribution of FRP obtained from the proposed model, considering the reinforcement ratio, and the shear contribution of FRP obtained from experimental results are depicted in Figure 4. It is seen that the proposed model reflects the $\rho_0$variation quite well when calculating the shear contribution of FRP.

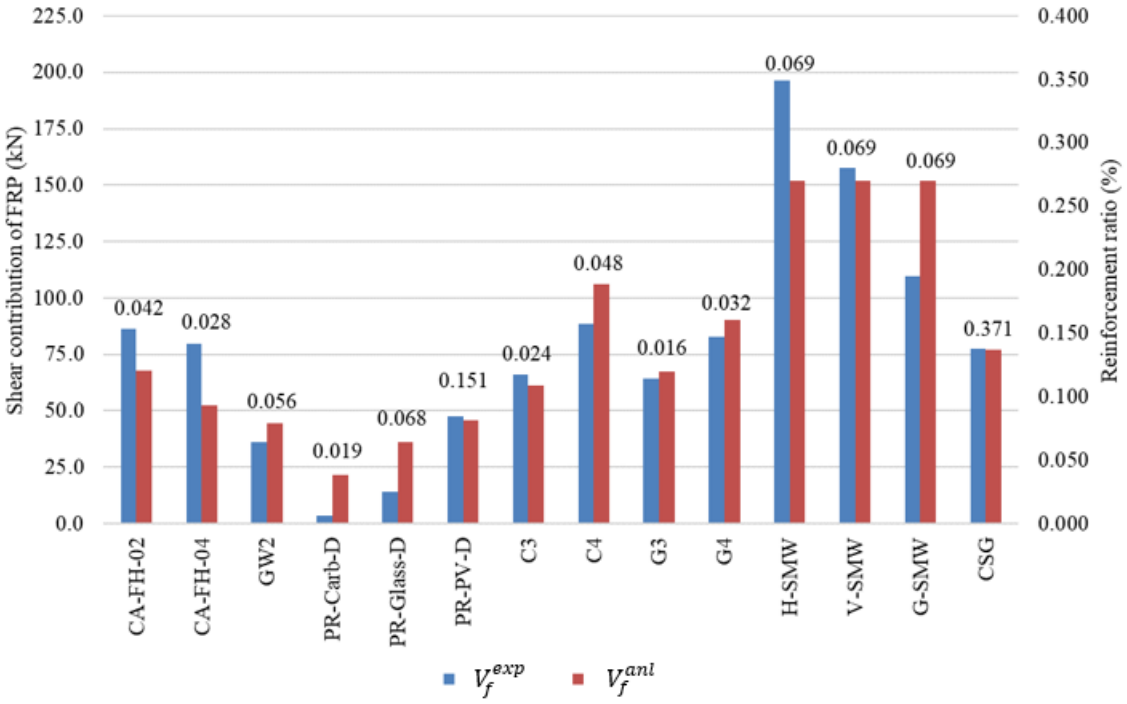

Figure 4. Variation in shear contribution of FRP considering reinforcement ratio

4. Conclusion

The primary focus of this study is to examine and analyze the shear contribution of FRP strips. Within the scope of the study, an experimental database was created by compiling studies in the literature on unreinforced masonry walls with different reinforcement configurations. Subsequently, a new empirical equation considering the effect of reinforcement ratio (ρ_0) is proposed to estimate the contribution of FRP strips to shear strength of unreinforced masonry walls by non-linear regression analysis in SPSS. The validity of the proposed empirical model was compared with the experimental results and the values predicted by ACI 440.7R-10 code.

In summary, the proposed model has a slightly higher capability to predict experimental outcomes compared to the ACI-440.7R-10 model. Furthermore, since ρ_0 is considered in the proposed model, unlike the ACI-440.7R-10 code, the proposed model better reflected the derivations in the experimentally obtained shear strength capacity due to the change of the ρ_0. The observation reveals that the suggested model accurately anticipates the shear strength capabilities of the walls having the highest and lowest ρ_0 values in the dataset. Several unresolved inquiries remain concerning the in-plane behavior of both reinforced and unreinforced masonry walls. In future research, it may be worthwhile to develop robust analytical models able to forecast nominal shear strength capacity of strengthened URM walls. This could be accomplished through the utilization of a comprehensive experimental dataset.

5. References

ACI 440.7R-10, 2010, Guide for the design and construction of externally bonded FRP system for strengthening unreinforced masonry structures, American Concrete Institute.

Cheng, S., Yin, S., Jing, L., 2020. Comparative experimental analysis on the in-plane shear performance of brick masonry walls strengthened with different fiber reinforced materials. Construction and Building Materials, 259, 120387.

CNR-DT 200, 2004, Guide for the design and construction of externally bonded FRP systems for strengthening existing structures, Advisory Committee on Technical Recommendations for Construction.

Doran, B., Ulukaya, S., Unsal Aslan, Z., Karslioglu, M., Yuzer, N., 2021. Experimental Investigation of CFRP Strengthened Unreinforced Masonry Walls with Openings. International Journal of Architectural Heritage.

Elgawady, M. A., Lestuzzi, P., Badoux, M., 2004. A review of conventional seismic retrofitting techniques for URM. 13th International Brick and Block Masonry Conference, 1–10.

ElGawady, M., Lestuzzi, P., Badoux, M., 2004. A review of retrofitting of unreinforced masonry walls using composites. 4th International Conference on Advanced Composite Materials in Bridges and Structures, July, 1–8.

Emami, M., Eftekhar, M. R., Karimizadeh, H., 2018. Experimental study on postponing the deboning of FRP sheets in masonry walls. International Journal of Architectural Heritage.

Garbin, E., Galati, N., Nanni, A., Modena, C., Valluzzi, M. R., 2007. Provisional design guidelines for the strengthening of masonry structures subject to in-plane loading. 10th North American Masonry Conference, 458–471.

Marcari, G., Manfredi, G., Prota, A., Pecce, M., 2007. In-plane shear performance of masonry panels strengthened with FRP. Composites Part B: Engineering, 38(7–8), 887–901.

Marcari, G., Oliveira, D. V., Fabbrocino, G., Loureno, P. B., 2011. Shear capacity assessment of tuff panels strengthened with FRP diagonal layout. Composites Part B: Engineering, 42(7), 1956–1965.

Maria, H. S., Alcaino, P., Luders, C., 2006. Experimental response of masonry walls externally reinforced with carbon fiber fabrics. 8th US National Conference on Earthquake Engineering 2006, 14(February 2014), 8555–8564.

Marshall, O. S., Sweeney, S. C., Trovillion, J. C., 2000. Performance testing of fiber-reinforced polymer composite overlays for seismic rehabilitation of unreinforced masonry walls.

Martinelli, E., Perri, F., Sguazzo, C., Faella, C., 2016. Cyclic shear-compression tests on masonry walls strengthened with alternative configurations of CFRP strips. Bulletin of Earthquake Engineering, 14(6), 1695–1720.

Moon, F. L., Yi, T., Leon, R. T., Kahn, L. F., 2007. Testing of a Full-Scale Unreinforced Masonry Building Following Seismic Strengthening. Journal of Structural Engineering, 133(9), 1215–1226.

Rahman, A., and Ueda, T., 2016. In-Plane Shear Performance of Masonry Walls after Strengthening by Two Different FRPs. Journal of Composites for Construction, 20(5), 1–14.

Triantafillou, T., and Antonopoulos, P., 1999. Design of Concrete Flexural Members Strengthened in Shear With FRP. ASCE Journal of Materials in Civil Engineering, 11(4), 325–330.

Triantafillou, T. C., 1998. Strengthening of Masonry Structures Using Epoxy-Bonded FRP Laminates. Journal of Composites for Construction, 2(2), 96–104.

Valluzzi, M. R., Tinazzi, D., Modena, C., 2002. Shear behavior of masonry panels strengthened by FRP laminates. Construction and Building Materials, 16(7), 409–416.

Vega, C., Torres, N., 2018. External strengthening of unreinforced masonry walls with polymers reinforced with carbon fiber. Ingeniería e Investigación, 38(3), 15-23.

Wang, Q., Chai, Z., Huang, Y., Yang, Y., Zhang, Y., 2006. Seismic shear capacity of brick masonry wall reinforced by GFRP. Asian Journal of Civil Engineering (Building and Housing), 7(6), 563–580.